water

MDPI

Article

Viscosity Controls Rapid Infiltration and Drainage, Not the Macropores

Peter Germann

Faculty of Science, Institute of Geography, University of Bern, 3012 Bern, Switzerland; pf.germann@bluewin.ch

Received: 12 November 2019; Accepted: 20 January 2020; Published: 24 January 2020

Abstract: The paper argues that universal approaches to infiltration and drainage in permeable media pivoting around capillarity and leading to dual porosity, non-equilibrium, or preferential flow need to be replaced by a dual process approach. One process has to account for relatively fast infiltration and drainage based on Newton's viscous shear flow, while the other one draws from capillarity and is responsible for storage and relatively slow redistribution of soil water. Already in the second half of the 19th Century were two separate processes postulated, however, Buckingham's and Richards' apparent universal capillarity-based approaches to the flow and storage of water in soils dominated. The paper introduces the basics of Newton's shear flow in permeable media. It then presents experimental applications, and explores the relationships of Newton's shear flow with Darcy's law, Forchheimer's and Richards' equations, and finally extends to the transport of solutes and particles.

Keywords: wetting shock fronts; shear flow; viscosity; capillarity; kinematic waves

1. Introduction

Infiltration is the transgression of liquid water from above the surface of the permeable lithosphere to its interior, while drainage refers to liquid water leaving some of its bulk. For example, within about three weeks after liquid manure applications, bad odors appeared in drinking water wells at depths between 10 to 50 m in English Chalk [1]. In the same geological formations, the annual surplus of the water balance moved down with about 1 m year^{-1} as profiles of isotope ratios of $^{18}O/^{16}O$ revealed [2]. The contrasting observations lead to ratios between 150 and 700 of the velocities of the 'odor' front vs. the isotope front that illustrate well the difference between rapid and slow infiltration.

Fast flow and transport are usually attributed to preferential flow in the macropore domain, while slower movements are supposedly due to flow in the capillary domain as expressed with Richards' [3], allowing for exchanges between the two domains as, for instance [4] and [5] have recently compiled. This contribution favors a dual-process approach to infiltration and drainage over dual-porosity approaches, thus avoiding the a-priori delineation between 'macropores' and the remaining porosity.

Beginning in the middle of nineteenth century, the next section summarizes the evolution of permeable media flow concepts for both, saturated and unsaturated flows. The third section provides the base for Newton's shear flow, stressing vertical viscous flow during rapid infiltration, while capillarity is assigned to the much slower redistribution of soil moisture but in all directions. The fourth section provides experimental evidence, and is followed by the conclusions.

2. Evolution of Infiltration and Drainage Concepts

This section provides some milestones on the way to a dual-process approach to infiltration and drainage, where Newton's shear flow covers fast and gravity driven flows, while Richards' capillary flow is considered to deal mainly with slower capillary rises and redistributions. By no means is this section intended to cover the history of infiltration and drainage.

2.1. Steady Saturated Flow

In the mid-19th century, there was an increasing interest in flows in saturated soils and similarly permeable media. Hagen, a German hydraulic engineer, and Poiseuille (1846) [6] a French physiologist, independently analyzed laminar flow in thin capillary tubes. Darcy (1856) [7], in the quest of designing a technical filtration system for the city of Dijon, empirically developed the concept of hydraulic conductivity as proportionality factor of flow's linear dependence on the pressure gradient. Dupuit (1863) [8] expanded Darcy's law to two dimensions as perpendicular and radial flow between two parallel drainage ditches and towards a groundwater well, respectively. Forchheimer (1901) [9] added an expression to Darcy's law that accounts for high pressures, steep gradients, and high flow velocities in the liquid.

2.2. Early Studies on Flow in Unsaturated Soils

Schumacher (1864) [10], a German agronomist, was probably the first who considered capillarity as the cause for simultaneous flows of water and air in partially water-saturated soils. He qualitatively compared the rise of wetting fronts in soil columns with the rise of water in capillary-sized glass tubes, and concluded that the wetting fronts rise higher but slower in finer textured soils compared with coarser materials. He also infiltrated water in columns of undisturbed soil and found that infiltration fronts progressed much faster than the rising wetting fronts. He suggested two separate processes for the two flow types: (i) slower capillary rise and (ii) faster infiltration, however, without further dwelling on the latter. Lawes et al. (1882) [11] concluded from the chemical composition of the drain from large lysimeters at the Rothamsted Research Station that "The drainage water of a soil may thus be of two kinds (1) of rainwater that has passed with but little change in composition down the open channels of the soil; or (2) of the water discharged from the pores of a saturated soil." [11] prioritized two separate flow paths to explain the observations.

2.3. Universal Capillary Flow in Unsaturated Soils

During the second half of the 19th century, modern irrigation agriculture spread in semi-arid areas, thus increasing the demand for better understanding the soil-water regime. Buckingham (1907) [12], working on a universal approach to the simultaneous storage and flow of water and air in soils, postulated the relationship between the capillary potential ψ Pa and the volumetric water content θ m^3 m^{-3}, also known as the water retention function, retention curve, or water release curve. The capillary potential follows from the Young–Laplace (1805) [13] relationship, stating that the pressure difference between a liquid and the adjacent gas phase increases inversely proportional to the radius of the interface. Capillary potential emerges as energy per unit volume of water in the permeable medium due to the water's surface tension. Canceling energy and volume with one length leads to force per area. Because the menisci's surfaces are bent into the liquid, $\psi < 0$, where $\psi = 0$ corresponds to the air pressure as reference. In addition to the specific weight of the soil water, [12] introduced the spatial gradient of ψ as the other major driving force. Besides infiltration, this stroke of a genius accounts for the redistribution of soil water in all directions, evaporation across the soil surface, transpiration via roots, and capillary rise from perched water including groundwater tables. In analogy to Fourier's (1822) [14] and Ohm's (1825) [15] laws for heat flow and electrical current, and Darcy's law for water flow in saturated porous media, [12]postulated the hydraulic conductivity for flow in unsaturated porous media as function of either $K(\theta)$ or $K(\psi)$ m s^{-1}. According to Or (2018) [16], the British meteorologist Richardson (1922) [17] was most likely the first who introduced a diffusion type of K-ψ-θ-relationship in the quest of quantifying water exchange between the

atmosphere and the soil as lower boundary of the meteorological system. A second-order partial differential expression became necessary because ψ depends on θ, and both their temporal variations on flow, while flow itself is driven by the gradient of ψ.

The race was on to the experimental determination of the *K*-ψ-θ-relationships. For instance, Gardner et al. (1922) [18] used plates and blocks of fired clay with water-saturated pores fine enough to hydraulically connect the capillary-bound water within soil samples with systems outside them. [3] applied the technique to the construction of tensiometers that directly measure ψ within an approximate range of $0 > \psi >\approx -80$ kPa. With the pressure plate apparatus he measured ψ-θ-relationships and determined hydraulic conductivity *K*(ψ or θ). Similar to [17], he presented a diffusion-type approach to the transient water flow in unsaturated soils. Numerous analytical procedures evolved for solving the Richards equation, among them a prominent series of papers by J.R. Philip [19]. Moreover, van Genuchten (1980) [20] developed mathematically closed forms of *K*-*ψ*-*θ*-relationships that provide the base for the many hues of HYDRUS i.e., various numerical simulation packages dealing with flow and storage of water and solutes in unsaturated soils (Simunek et al., 1999, [21]).

2.4. Early Alternatives to Universal Capillary Flow

In his quest of demonstrating the benefit of forests and reforestations on controlling floods and debris flows from steep catchments in the Swiss Alps and Pre-Alps, Burger (1922) [22] measured in situ the time lapses Δt_{100} for the infiltration of 100 mm of water into soil columns of the same length. In the laboratory, he determined the air capacity *AC* m^3 m^{-3} of undisturbed samples collected near the infiltration measurements, where *AC* is the difference of the specific water volume after standardized drainage on a gravel bed and complete saturation.

Veihmeyer (1927) [23] investigated water storage in soils with the aim of scheduling irrigation. He proposed the water contents at field capacity (FC) and at the permanent wilting point (PWP) as upper and lower thresholds of plant-available soil water. Free drainage establishes FC a couple of days after a soil was saturated and evapo-transpiration was prevented. The water loss before achieving FC is referred to as 'drainable' or 'gravitational' soil water. PWP is considered θ at $\psi = -150$ kPa (= −15 bar).

2.5. Dual Porosity Approaches

It became unavoidable that concepts based on Buckingham's (1907) [12] fundamental and seminal work contradicted with practical and field-oriented research. Veihmeyer (1954) [24], for instance, stated "Since the distinction between capillary and other 'kinds' of water in soils cannot be made with exactness, obviously a term such as non-capillary porosity cannot be defined precisely since by definition it is determined by the amount of 'capillary' water in the soils". Additionally, progress in field instrumentation as well as in computing techniques allowed for producing and processing large data sets including the numerical solution of Richards equation. In the late 1970s, the development increasingly unveiled substantial discrepancies between measurements and the numerous approaches to water movement in unsaturated soils based on [3] capillarity-dominated theory. Particularly disturbing were observations on wetting fronts advancing much faster than expected from the Richards approach.

The mid-1970s initiated the thread of dual-porosity approaches to preferential flows. Bouma et al. (1977) [25] were among the first to introduce the term macropores in view of non-equilibrium in *ψ*-*θ*-relationships, while the compilation by Beven and Germann (1982) [26] on the subject is still referred to today. The discussion has gradually moved from macropore flow to preferential flow that summarizes all the flows in unsaturated porous media not obeying the Richards equation [4]. Numerous reviews on macropore flows, preferential flows, non-equilibrium flows, and non-uniform flows in permeable media appear periodically, and only the latest are here referenced [5,27].

Beven (2018) [28] argued that, for about a century, the hardly questioned preference given to capillarity denied recognition of concepts considering flow along macropores, pipes, and cracks. Indeed, there is an increasing number of contributions focusing on the dimensions and shapes of flow

paths, their 3-D imaging, and trials to derive flows from them [4]. However, there is hardly an approach capable of applying the wealth of information about the paths to the quantification of flow. Ignoring Veihmeyer's (1954) [23] warning, the attraction of research on flow paths is so dominant that, for instance, Jarvis et al. (2016) [4] flatly denied the applicability of Hagen–Poiseuille concepts to flow in soils. Moreover, advanced techniques of infiltration with non-Newtonian fluids led so far just to the description of path structures rather than more directly to the flow process [29]. Widespread research in the types, dimensions, and shapes of 'macropores' and their apparent relationships to flow and transport mostly pivot around Richards equation that is numerically applied to either macropore-/micropore-domains or by modelling flow and solute transport in the macropore domain with separate rules yet still maintaining a Richards-type approach to micropore-flow. Both types of approaches allow for exchanges of flow and solutes between the two domains. Imaging procedures visualize flow in 2-D and 3-D in voids as narrow as some 10 μm, rising hope that the wealth of information gained so far at the hydro-dynamic scale will eventually lead to macroscopic models at the soil profile scale of meters [4]. Thus, Beven's (2018) [28] denial of progress in infiltration research is here carried a step further. The obsession with pores, channels, flow paths, and their connectivity, tortuosity, and necks actually retarded research progress towards more general infiltration that has to be based on hydro-mechanical principles.

2.6. Early Search for Alternatives

The alternative approach should be based on the same principles as Hagen–Poiseuille's and Darcy's laws, whereas Newton's (1729) [30] shear flow (Nsf) appears as a solid and suitable foundation. The approach then should close the gap of one to two orders of magnitude of hydraulic conductivity between saturated flow and flow close to saturation [31].

Unearthing Burger's (1922) [22] data, [32] found an encouraging coefficient of determination of $r^2 = 0.77$ when correlating via a Hagen–Poiseuille approach 76 pairs of Δt_{100}- and AC-values. Beven and Germann (1981) [33] modelled laminar flow in tubes and planar cracks, and proposed kinematic wave theory according to Lighthill and Whitham (1955) [34] as analytical tool for handling Nsf. Germann (1985) [35] applied the theory successfully to data from an infiltration-drainage experiment carried out on a block of polyester consolidated coarse sand that experimentally support the flow-(q-) version of Nsf, where q m s^{-1} is volume flux density.

Dye experiments confirmed expectations, not the least by purposefully setting the initial and boundary conditions. [36], for instance, demonstrated preferential flow along earthworm burrows down to the 0.4 m depth as well as radially away from the channels by inundating with rhodamine dye and a bromide solution the tops of columns of undisturbed soil. Following [11], who reported fast drainage, Germann (1986) [37] assessed the arrival times of precipitation fronts in the Coshocton lysimeters. Accordingly, rains of 10 mm d^{-1} sufficed to initiate or increase drainage flow within 24 h at the 2.4 m depth when θ in the upper 1.0 m of the soil was at or above 0.3 m^3 m^{-3}. The observations result in wetting front velocities greater than 3×10^{-5} m s^{-1}.

2.7. Development of Newton's Shear Flow Approach to Infiltration and Drainage

The advent of TDR- and data recording techniques fostered the water-content-(w-) version of Nsf (where w m^3 m^{-3} refers to the mobile water content) applicable to in-situ infiltration experiments using controlled sprinkler irrigation and producing time series of θ at various depths in soil profiles. Discussions with L. Dipietro and V. P. Singh linked experiments with basic concepts [38]. Investigations of acoustic velocities across a column of an undisturbed soil during infiltrations, [39] proved independently from the capillarity narrative that rapidly infiltrating water is under atmospheric pressure. Originally, macropore flow was the prominent research topic. Shortfalls of the capillarity-dominated concepts emerged when juxtaposed to matured Nsf-versions [40]. Hence, this paper is the première of consequently carrying through the dual-process approach to infiltration and drainage.

There were projects leading off the track. [41], for instance, proposed a kinematic wave approach to infiltration that included a sink function accounting for water abstraction from the moving to the

sessile parts. Later rigorous testing of the approach against real data unveiled the misconception. Additionally, [42] superimposed a bundle of rivulets to model data. That again turned out as impracticable. [43] were looking for FC in soil profiles after the cessation of infiltration. However, repeated experiments showed quite variations in expected constant final FCs.

2.8. State of Nsf

Gradually, some of the subordinate concepts lined out above get referenced. However, as of yet, outside the author's immediate environment of research, there is hardly an elaborated application of Nsf to infiltration and drainage. Unavoidably, this leads to the impression of self-indulgence, particularly in view of the paper's lopsided list of references. The Guest Editor's invitation to its submission may ease the charge. Moreover, although [26] mainly outlined the need for research on 'macropore flow' and did not offer much of research guidance, that paper is still frequently referenced, indicating that researchers have hardly agreed on a basic approach to the problem as they did and still do, for instance, on the Richards equation.

3. Newton's Shear Flow in Permeable Media

The section summarizes the basics of Newton's shear flow (Nsf) in permeable media. Detailed derivations of the relationships have previously been published [44–46], thus only the major expressions are here presented. The approach is laid out at the hydro-mechanical scale of spatio-temporal process integration, allowing for its easy handling with analytical expressions, yet under strict observance of the balances of energy, momentum, and mass (i.e., the continuity requirements).

The interior of a permeable solid medium contains connected flow paths that are wide enough to let liquids pass across its considered volume. The definition purposefully avoids further specification of the flow paths' shapes and dimensions. Water supply to the surface is thought of a pulse $P(q_S,T_B,T_E)$, where q_S m s^{-1} is constant volume flux density from the pulse's beginning at T_B to its ending at T_E, both s. (The subscript S refers to the surface of the permeable medium). The pulse initiates a water content wave (*WCW*) of mobile water that is conceptualized as a film gliding down the paths of a permeable medium according to the rules of Newton's shear flow. The *WCW* is the basic unit of shear flow whose hydro-mechanical properties are going to be presented below.

Referring to Figure 1, the parameters film thickness F m and specific contact length L m m^{-2} per unit cross-sectional area A m^2 of the medium specify a *WCW*. Regardless of the thickness of F, atmospheric pressure prevails within the film. A *WCW* supposedly runs along the flow paths while forming a discontinuous and sharp wetting shock front at $z_W(t)$. The *WCW* partially fills the voids of the upper part of the medium within $0 \le z \le z_W(t)$ with the mobile water content $w(z,t)$ m^3 m^{-3}, where $w \le \varepsilon - \theta_{ante}$, where ε and θ_{ante} are porosity and antecedent θ, respectively, both m^3 m^{-3}. The lower part $z > z_W(t)$ remains at θ_{ante}. The coordinate z m originates at the surface and points positively down. The water film of the *WCW* consists of an assembly of parallel laminae, each df m thick and moving with the celerity of $c(f)$ m s^{-1}. Celerity refers to the wave velocity, for instance of a lamina. Newton (1729) [30] defined viscosity as "The resistance, arising from the want of lubricity in the parts of a fluid, is, caeteris paribus, proportional to the velocity with which the parts of the fluid are separated from each other." In our case, the definition translates to the shear stress $\varphi(f)$ Pa in the unit area of $L \times A \times z_W(t)$ m^2 per unit volume $A \times z_w(t)$ m^3 of the medium at distance $0 \le f \le F$ m from the soil-water interface (*SWI*), acting in the direction opposite to gravity. $\varphi(f)$ balances the weight of the film from f to F. Integration of the shear stress balance from 0 to f under consideration of the non-slip condition of $c(0) = 0$ leads to the parabolic celerity profile of the laminae within the film. The differential flow of a lamina is $dq(f) = L \times c(f) \times d(f)$. Its integration from 0 to F i.e., from the *SWI* to the air-water interface (*AWI*), leads to the volume flux density of the entire film as:

$$q(F,L) = \frac{g}{3 \cdot \eta} \cdot L \cdot F^3 \quad (1)$$

m s^{-1}, where g (= 9.81 m s^{-2}) is acceleration due to gravity and η (≈10^{-6} m^2 s^{-1}) is temperature-dependent kinematic viscosity. The volume of mobile water per unit volume of the permeable medium from the surface to $z_W(t)$ amounts to:

$$w(F, L) = F \cdot L \tag{2}$$

m^3 m^{-3}. The constant velocity of the wetting shock front follows from the volume balance as:

$$v_W(F) = \frac{q(F, L)}{w(F, L)} = \frac{g}{3 \cdot \eta} \cdot F^2 \tag{3}$$

Thus, the position of the wetting shock front as function of time becomes:

$$z_W(t) = v_W \cdot (t - T_B) = (t - T_B) \cdot \frac{g}{3 \cdot \eta} \cdot F^2 \tag{4}$$

m s^{-1}. Accordingly, L m m^{-2} is not only the specific contact length of the film per A but, under consideration of $z_W(t)$, L m^2 m^{-3} evolves as the specific vertical contact area of the *WCW* with the sessile parts of the permeable medium per unit volume. It thus turns into the locus of exchange of momentum, heat, capillary potential, water, solutes, and particles between the *WCW* and the sessile parts of the medium.

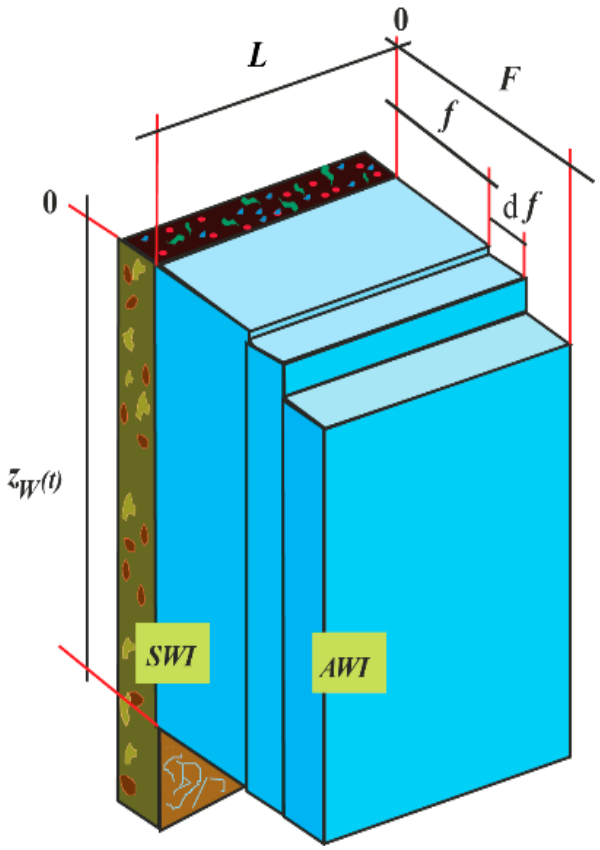

Figure 1. Film flow along a vertical plane, where F m is the film thickness, f m is the thickness variable, df m is the thickness of a lamina, $z_W(t)$ m is the vertical position of the wetting shock front as function of time t s, and L m m^{-2} is the specific contact length between the moving water film and the sessile parts of the permeable medium per its unit horizontal cross-sectional area A m^2. *AWI* and *SWI* are the air-water and the solid-water interfaces, respectively. ([44]; with permission from the publisher).

Equations (1)–(4) hold during infiltration i.e., $T_B \le t \le T_E$. Input ends abruptly at T_E and at $z = 0$ i.e., $q_S \to 0$, when and where the *WCW* collapses from $f = F$ to $f = 0$. All the rear ends of the laminae are

released at once at $z = 0$. The outermost lamina moves the fastest with the celerity of the draining front as:

$$c_D = \frac{\mathrm{d}q(F)}{\mathrm{d}w} = \frac{\mathrm{d}q(F)}{L \cdot \mathrm{d}f} = \frac{g}{\eta} \cdot F^2 = 3 \cdot v_W \tag{5}$$

m s^{-1}. While v_W follows from the volume balance Equation (3), the three times faster c_D follows from the parabolic function $c(f)$ (see, for instance, Germann and Karlen, 2016). The outer most lamina moves with c_D also during $0 \le t \le T_E$. Therefore, the slower moving wetting shock front continuously intercepts the faster moving laminae. This results in a sharp wetting shock front at $z_W(t)$ with $\theta_{ante} + w$ between the surface and the wetting shock front and θ_{ante} ahead of it. The wetting shock front presents a discontinuity of the *WCW*. The rear end of the draining front that was released at T_E catches up with wetting shock front at time T_I s that follows from setting $v_W \times (T_I - T_B) = c_D \times (T_I - T_E)$ as

$$T_I = \frac{1}{2} \cdot (3 \cdot T_E - T_B) \tag{6}$$

Thus, T_I is exclusively an expression of the pulse duration. The wetting shock front intercepts the draining front at depth:

$$Z_I = (T_E - T_B) \cdot F^2 \cdot \frac{g}{2 \cdot \eta} \tag{7}$$

m. The two expressions T_I and Z_I represent the spatio-temporal scale of a *WCW*. The rear ends of all the other laminae move with decreased celebrities, ultimately leading to the spatio-temporal distribution of the mobile water content from the surface to the wetting shock front as:

$$w(z,t) = L \cdot \left(\frac{\eta}{g}\right)^{1/2} \cdot z^{1/2} \cdot (t - T_E)^{-1/2} \tag{8}$$

After T_I and beyond Z_I the draining front disappears and $v_W(z,t)$ decreases with time and depth, leading to the position of the wetting shock front as:

$$z_W(t) = \left(\frac{3 \cdot V_{WCW}}{2 \cdot L}\right)^{2/3} \cdot \left(\frac{g}{\eta}\right)^{1/3} \cdot (t - T_E)^{1/3} \tag{9}$$

with the mobile water content of:

$$w(t)\big|_{z_W} = \left(\frac{\eta}{g}\right)^{1/3} \cdot \left(\frac{3 \cdot V_{WCW}}{2}\right)^{1/3} \cdot (t - T_E)^{-1/3} \cdot L^{2/3} \tag{10}$$

while the volume flux density at the wetting shock front becomes:

$$q(t)\big|_{z_W} = \frac{V_{WCW}}{2 \cdot (t - T_E)} \tag{11}$$

where $V_{WCW} = q_S \times (T_E - T_B)$ m is the total volume of the *WCW*. Figure 2 illustrates the relationships describing a *WCW*.

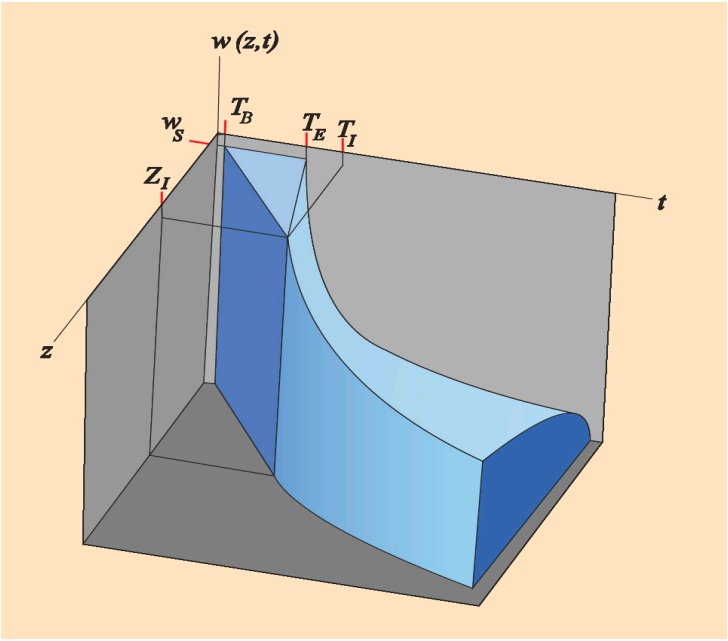

Figure 2. Schematic representation of a water-content wave *WCW*, where the $w(z,t)$-axis represents the mobile water content, t and z are the axes of time and depth; w_S indicates the mobile water content that follows from q_S; T_B and T_E s are the beginning and ending times of the water pulse $P(q_S, T_B, T_E)$ that hits the surface at $z = 0$; T_I and Z_I indicate time and depth of the wetting front intercepting the draining front. The wetting shock front continues beyond $t > T_I$ and $z > Z_I$ as curve along time and depth.([44]; with permission from the publisher).

A *WCW* i.e., $w(z,t)$,translates easily into a volume flux density wave according to:

$$q(z,t) = b \cdot w(z,t)^3 \tag{12}$$

with $b = g/\left(3 \cdot L^2 \cdot \eta\right)$ m s^{-1}. The approach applies to laminar flow as assessed with the Reynolds number:

$$Re = \frac{F \cdot v}{\eta} = \frac{F^3 \cdot g}{3 \cdot \eta^2} = \left(\frac{3 \cdot v^3}{g \cdot \eta}\right)^{1/2} \tag{13}$$

$Re \leq 1$ strictly defines laminar flow; however, depending on the application, $Re > 1$ might be tolerable, yet within an undisclosed range.

The parameters film thickness F m and specific contact area L m^2 m^{-3} of a *WCW* due to a pulse $P(q_S,T_B,T_E)$ follow from time series of either volumetric water contents $\theta(Z,t)$ or from volume flux density $q(Z,t)$, where Z (m) represents a specific depth in the permeable medium. Presumably, F and L get established shortly after T_B. Their sizes are due to q_S and the actual properties of the permeable medium, such as θ_{ante} and related flow paths supporting F and L. Predictions of F and L are currently undisclosed, thus restricting the approach to *a posteriori* data interpretation.

4. Examples

The section provides examples in support and as illustrations of Nsfa. More, and more elaborated examples are presented in [44].

4.1. Experimental Support of Newton's Shear Flow in Permeable Media

Constant wetting front velocities, Equation (3): Already [47] observed constant velocities of wetting fronts during finger flow in sandboxes down to the 0.9-m depth. [48] reported the same kind of observations over a depth range of 2 m during infiltration in the Kiel Sand Tank, while [49] found

constant wetting front velocities under natural precipitation regimes across the upper 1.5 m of the undisturbed soil in a large weighing lysimeter. With 34 FTDR-probes in three boreholes, [50] followed infiltration in an ancient sand dune in Israel. From their data, [44] deduced two constant wetting front velocities: one of about 5×10^{-6} m s^{-1} above the clay-rich layer at the 8-m depth, and one of about 2×10^{-6} m s^{-1} down to the 21 m depth. The two coefficients of determination (r^2) of the linear regressions of arrivals vs. depths of the wetting front amounted to 0.83 and 0.94, respectively. Constant wetting front velocities support the early stage of *WCW*s, Equation (3), and imply constant F.

Laminar flow: From more than 200 infiltration experiments, [51] reported a range of $10^{-5} < v_W < 2 \times 10^{-2}$ m s^{-1}. According to Equation (13), this leads to a range of $10^{-4} < Re < 1.6$. The upper limit is still close to laminar flow. In General, permissible upper limits of Re demand attention in view of the applicability of Nsf.

Atmospheric pressure behind wetting fronts: Atmospheric pressure in the *WCW* is a prerequisite of Nsf-theory. [48] antecedent capillary heads in the range from −1.2 to −0.8 m to collapse to about −0.2 m behind the wetting front. [42] found similar patterns of capillary-head collapses during infiltration into a column of a sandy-loam textured mollic Cambisol. Additionally, acoustic velocities during infiltration in a column of an undisturbed loess soil, [39] led [40] to the same conclusion of capillary head's break-up close to atmospheric pressure after the passing of the wetting front.

Cohesion of Newton's shear flow approach*:* The parameters F and L suffice to treat infiltration and drainage with Nsf, Equations (1) and (12). In principle, time series of either $\theta(Z,t)$ or $q(Z,t)$ permit calibration of the two parameters: [45] shows their calibration from $\theta(Z,t)$, while [47] provide the procedure from q-series. The latter authors and [44] also demonstrate the cohesion of the approach in that derivations from both time series resulted in the same amount of L.

4.2. Newton's Shear Flow vis-à-vis Darcy's Law and Forchheimer's Equation

Darcy's law mutates to the saturated-flow extension of unsaturated vertical shear flow under the following considerations. When replacing kinematic viscosity with the dynamic viscosity, $\mu = \rho \times \eta$, follows from Equation (1) that:

$$\theta_{ante} + w < \varepsilon \text{ and } \Delta p/\Delta z = \rho \times g \qquad q = \frac{F^3 L}{3 \mu} \rho g \tag{14}$$

where θ_{ante} m^{3}m^{-3} is the antecedent volumetric water content, ε m^{3}m^{-3} is porosity, $\Delta p/\Delta z$ Pa m^{-1} is the pressure gradient, ρ (= 1000 kg m^{-3}) is the density of water, and $\mu = \rho\, \eta$ Pa s is dynamic viscosity. At saturation we get:

$$\theta_{ante} + w = \varepsilon \text{ and } \Delta p/\Delta z = \rho \times g: \qquad q_{sat} = \frac{F_{sat}^3 L_{sat}}{3\mu} \rho g = K_{sat} \tag{15}$$

while an external pressure gradient leads to:

$$\theta_{ante} + w = \varepsilon \text{ and } \Delta p/\Delta z > \rho \times g: \qquad q(p) = \frac{F_{sat}^3 L_{sat}}{3\mu} \frac{\Delta p}{\Delta z} = q_{sat} \frac{\Delta p}{\Delta z \rho g} \tag{16}$$

Darcy's law states that q is proportional to $\Delta p/\Delta z$ i.e., volume flux density is a linear function of the flow-driving gradient with the proportionality factor K_{sat}. In view of the various dimensionalities of w proportional to (L^1, F^1), v proportional to (L^0, F^2), and q proportional to (L^1, F^3), linearity seems only possible if F_{sat} and L_{sat} remain constant and independent from p in the transition from only gravity-driven to pressure-driven shear flow at saturation i.e., in the transition from Equation (15) to Equation (16). The elaboration supports the linearity of Darcy's law, but it is not an independent proof of the law's linearity. As a consequence, $w = q/v$ also remains constant. Further, if $\theta_{ante} + w = \varepsilon$, $dL_{sat}/dp = 0$ and $dF_{sat}/dp = 0$ then follows the hypothesis that ($F_{sat} \times L_{sat}$) represent $(F \times L)_{max}$ leading to K_{sat}. However, other combinations of ($F \times L$) in unsaturated media are feasible that may lead to $q_{unsat} > q_{sat} = K_{sat}$. The presumption of $q_{unsat} > K_{sat}$ opens an new view on shear flow and the basics of infiltration that are in stark contrast to Richards' capillary flow, where a priori $K_{sat} > K(\theta \text{ or } \psi)$. Comparisons of the rates from field infiltration with K_{sat}-measurements in the laboratory vaguely support the presumption of [45] and [52] most recently provide experimental evidence of $q_{unsat} > K_{sat}$.

Atmospheric pressure prevails in a *WCW* in Newton's shear flow. However, parts of the the *WCW* may hit flow paths narrower than *F*, and $p > p_{atm}$ will occur. The difference $p > p_{atm}$ will dissipate almost instantaneously with the acoustic velocity in soil water between 300 and 800 m s^{-1} [53] if virtually no water has to be moved over short distances to the next path wider than *F*. However, increasing the distances between the paths that are wider than *F* leads to local pressure build up that may eventually lead to sessile water above a layer of reduced conductivity. Water saturation may occur from relatively short periods, for instance shortly after heavy rains, up to seasons as, for instance, mottles of chemically reduced and oxidized zones in soil profiles may illustrate. Drainage under $p > p_{atm}$ shows as a steeper recession than drainage under $p = p_{atm}$. [49] provide the details. [54] report $\theta(t)$-time series of TDR-measurements immediately above an impervious soil layer that deviates from those of free flow during infiltration and that indicates the evolution of sessile soil water.

Forchheimer (1901) [9] added a quadratic term to Darcy's law that accounts for momentum dissipation under high flow velocities that occur under high pressure gradients i.e.,

$$-\frac{dp}{dx} = \frac{\eta}{K} v + \frac{\rho}{k_2} v^2 \quad (17)$$

where *K* and k_2 represent hydraulic conductivity and turbulence, respectivly. Neither of the two conditions apply to Nsf in unsaturated permeable media in the lithosphere near its interface with the atmosphere. Moreover, [54] estimate the relative contribution of kinetic energy in the range of 10^{-6} to 10^{-4} in comparison with viscous momentum dissipation during flow in soils. Thus, Forchheimer's equation does not apply to Nsf.

4.3. Gravity and Capillarity

Gravity is the unique driving force in Newton's shear flow in unsaturated permeable media, while capillarity is responsible for the soil water's redistribution and vertical rise from saturated zones. [10] suggested a two-process approach to water flow and storage in partially saturated permeable media. While he recognized capillarity as responsible for the water's rise, and probably also its contribution to water redistribution in soil columns, he left open the mechanism behind infiltration. Here, the focus is on infiltration that is completely gravity-driven and viscosity-controlled, yet allowing for water abstraction due to capillarity from the mobile to the immobile part of the permeable system. Richards' universal equation for flow and storage in unsaturated porous media revolves around capillarity. It prominently, and unnecessarily, reduces the degrees of freedom of flow [39]. Unjustified, it relates the coefficient of momentum dissipation with antecedent flow conditions i.e., $K(\theta$ or $\psi)$, thus a priori excluding atmospheric pressure in the moving water. The exclusion leads to too slow advancements of wetting as Germann and Hensel (2006) [55] have demonstrated by comparing the results from HYDRUS-2 model [21] performances with observed infiltrations from more than 200 sites. Concentrating on gravity and viscosity liberates infiltration and drainage from the omnipresence of capillarity in soil hydrology with the benefit of avoiding the difficult definitions of non-equilibrium flow and the separation of macropores from the remaining pores. With respect to capillarity, the relative contribution of gravity to flow varies according to *cos* (α), where $\alpha°$ is the angle of deviation from the vertical. Thus, at *cos* (0°) = 1, as in the cases presented above, gravity's contribution is at maximum; it reduces to *cos* (90°) = *cos* (270°) = 0, while it completely opposes capillarity at *cos* (180°) = −1. The juxtaposition illustrates the spatial limitations of Nsf. Moreover, lateral rapid flow requires saturated conditions along a layer with path widths narrower than *F*.

Pressure in the *WCW* is atmospheric while $\psi < 0$ typically prevails ahead of it. Therefore, water is abstracted from the *WCW* onto *L*. Abstraction is usually completed during short periods. The amount of abstraction shows in the difference between θ_{end}, when the *WCW* has ceased, and θ_{ante} before the passing of the *WCW*. θ_{end} is approached with Equation (8) for a particular depth *Z*, while setting the *WCW*'s end at $w(Z,t)/w_s = u$, where $u << 1$ is an arbitrarily selected threshold that depends on the particular application of Newton's shear flow. Water abstracted from the *WCW* is thus available for redistribution and uptake by plant roots.

4.4. Scales

The process scale during Nsf with constant F and L follows from the time and depth of interception, T_I and Z_I, Equations (6) and (7) that depend on the duration ($T_E - T_B$) of the input and on F. The velocity of the wetting shock front reduces after T_I and beyond Z_I according to Equation (9) [48].

The system-related scales of the applicability of Nsf range from a couple of sand grains at the mm-scale to the km-scale. From neutron radiographs taken during infiltration in sand boxes, Hincapié and Germann (2010)[56] calculated fluxes in layers that were about 1 mm thick and volume balances in the cm^3-range. Flow across 21 vertical m of an ancient sand dune was already presented above [49], while tracer experiment across crystalline rocks suggests the applicability of Newton's shear flow approach to the km-range. Dubois (1991) [57] injected the tracers uranin and eosin about 1800 m above the Mont Blanc car tunnel that connects Chamonix (France) with Courmayeur (Italy). Within 108 d he detected the tracer fronts in seeps in the car tunnel. This amounts to $v_W \approx 2 \times 10^{-4}$ m s^{-1} that is well within the range of the v_W-collection reported above. Moreover, the gentle water seeps in the tunnel revealed that gravity was consumed by viscosity during the long-lasting flow.

The observations of [57] across 1800 m of crystalline rocks of the Mont Blanc massif and the water balance calculations of finger flow in the sand boxes of [56] at the scale of millimeters hint at the spatial tolerance of Newton's shear flow. This may advance the approach to an attractive tool, for instance, for the study of infiltration into groundwater systems.

4.5. Time-Variable Infiltration

So far input to the surface is considered a single pulse $P(q_S, T_B, T_E)$. Time variable input needs to be separated into a series of rectangular pulses each carrying its individual parameters. Under the assumption of the macropore flow restriction i.e., $dL/dq = 0$, a series of pulses can be routed as a sequence of kinematic waves according [30],whose mathematical approach models Newton's shear flow correctly if $a = 3$ in Equation (12). [58] provides details of applying characteristics to the multi-pulse infiltration, while [49] lists some results.

Upon observations of infiltrations with varying durations and the rates from 5, to 10, 20, and 40 mm h^{-1} into a column of an undisturbed soil,[59] postulated the macropore flow restriction of $dL/dq_S = 0$, meaning that flow occurs along the same paths independently from the input rate. They tested the relationship of $v_W(q_S) = b^{1/3} \times q_S^{2/3}$, Equations (1) to Equation (3), that resulted in an acceptable coefficient of determination of $r^2 = 0.95$. However, that was an exception hardly achieved again. This calls for further investigation of the relationship, most likely under consideration of θ_{ante}.

4.6. Transport of Tracers and Particles

Preferential flow in soil hydrology is frequently associated with enhanced and accelerated particle, solute and, primarily, pollutant breakthrough [60]. However, Bogner and Germann (2019) [61] report considerable delays of tracer breakthrough compared with the first arrival of wetting shock fronts at the drain of soil columns with heights of 0.4 m. They referred to the phenomenon as 'pushing out old water' that is well known in catchment hydrology. They statistically explained 81% of the observed delay variations with combinations of L and F when applying Newton's shear flow to the data. It appears that tracer exchange on large L from thin F of the *WCW* may be even faster than presumed 'preferential' tracer transport. Under consideration of the mechanistic parameters F and L, Newton's shear flow provides for a novel tool for the unambiguous investigation of tracer transport and exchange i.e., accelerated as well as decelerated breakthroughs that primarily addresses the tracer's mass balance and secondarily diffusion.

Similar considerations may apply to the transport of particles and microbes. Based on a precursor of Nsf, [62] approached with drag-forces the transport of latex beads and bacteriophages in soils. The three types of electrically uncharged latex beads had dimeters of 0.5, 1.0, and 1.75 μm. Maximal particle concentrations relative to the input suspensions reached about 0.003. While the relationships between relative particle concentrations vs. drag force showed intermediate to strong

linearity during the increasing and decreasing limbs of the drain hydrograph, the drag force in the trailing was apparently too small to produce a considerable effect on their translocations. The five bacteriophages H40/l, H4/4, T7, H6/l, and fl carried ζ-potentials in the range of −50.1 to −31.7 mV. Their much weaker relative concentrations vs. drag force showed pronounced, yet undisclosed hysteresis. Recently, [63] called for improving our understanding of the transport of microplastic particles in soils, while [64] found these particles in worm burrows and assumed preferential flow along macropores as the major transport process. Thus, it might be worthwhile to further develop Newton's shear flow application to the particle transport under particular attention of the films thickness *F* and their specific contact areas *L*.

4.7. Ecohydrology

The early 20th century saw numerous runoff studies in headwater catchments, many of them with the purpose of demonstrating the advantage of forests over open lands in the mitigation of flood and debris flows from steep slopes, mainly to convince governments for subsidizing huge reforestation projects. Burger's (1922) [22] investigations with soil cores as well as his comparative runoff measurements from the 50% forested watershed of Rappengraben vs. the completely forested catchment of Sperbelgraben are well known in forest hydrology. However, not all the compartments from precipitation to runoff got the necessary attention in research they would require for closing the water balance. For instance, the infiltration experiments of [22] were not carried through to assess with them drainage and runoff in the headwater catchments.

Issues of reforestations' remedial effects on poorly permeable clay soils at sites in the Swiss pre-alps have surfaced again because numerous sites require rejuvenation of the more than 100 y old stands. In this context, Lange et al. (2009) [65] were able to demonstrate positive effects of tree root density on rapid infiltration in stagnic soils.

Wiekenkamp et al. (2019) [66] compared in the Wüstebach (BRD) catchment the hydrology of a forest site with the neighboring clear-cut site. They concluded that infiltration via preferential flow paths increased after deforestation. However, their purposeful exclusion of interception may deprive them of further interpreting the difference between the two treatments in rapid infiltration because interception may turn out as major gate controlling the input pulses $P(q_S, T_B, T_E)$.

5. Summary and Conclusions

The first section reports from English chalk rapid contaminant transport about 150 to 700 faster than the slow tracer movements. The second section deals with the evolution of infiltration-drainage concepts since the mid-19th Century. Two lines of thought emerge: On the one hand, Schumacher (1864) [10] suggested a two-processes approach for flow and storage of water in soils, one accounting for infiltration, the other one for capillary flow. On the other hand, a dual-porosity approach follows from the observations of Lawes et al. (1882) [11]. In searching an universal approach for storage and flow of water in partially saturated soils, Buckingham (1907) [12] and Richards (1931) [3] focused on capillarity and the soil hydrological functions K-θ-ψ. Concepts of non-equilibrium flow emerged upon discovered discrepancies between theory and observations that led later on to dual-porosity approaches. The third section takes off from Schumacher's two-processes approach, exploring fast infiltration and drainage as gravity-driven and viscosity controlled flow, resulting in a water content wave, *WCW*, that is based on Newton's shear flow i.e., laminar flow in unsaturated permeable media lasting two to ten times longer than the duration of input and occurring under atmospheric pressure. This restriction suggests strong capillary gradients between the *WCW* and the sessile parts. Because of the wide specific contact area, expressed with the factor *L* in the typical range of 500 to 20,000 m^2 m^{-3}, and the thin films *F* that are typically between 2 and 50 μm thick, exchanges of water, energy, heat, solutes, and particles are fast and strong. The fourth section elucidates applications of the approach.

On the one side, the universal Richards equation deals with infiltration and redistribution of soil water. It assumes that entire soil moisture θ participates in the flow process, thus inevitably leading to apparent conditions of non-equilibrium, while dual-porosity approaches are hoped to lead away

from the uneasy situation. On the other side, Newton's shear flow focuses on viscosity and gravity resulting in adequate time scales during infiltration and associated drainage. Once the wetting shock fronts have ceased to advance, capillarity takes over and soil moisture redistributes towards ψ-θ equilibria. This leads to a dual-process approach to infiltration and redistribution, where time and depth of front interception, T_I and Z_I, serve as scales for separating the two processes. A further consequence of concentrating flow and transport on Newton's shear flow are the spatio-temporal limits of the processes, expressed with a few multiples of T_I and Z_I. Moreover,' pushing out old water' and assuming flow rates under atmospheric pressure exceeding K_{sat} indicate novel aspects associated with Newton's infiltration that were not considerable in previous approaches to preferential flows. Finally, the analytical expressions are amenable to mathematical procedures, such as kinematic wave theory, and their theoretical combinations may lead to new and solid hypotheses calling for experimental testing.

Author Contributions: Conceptualization, methodology, formal analysis, investigation, writing—original draft preparation, review and editing, and supervision by P.F. The author has read and agreed to the published version of the manuscript.

Funding: This research did not receive any external funding

Acknowledgments: I thank Scholle, Guest Editor of the Special Issue on "Physical and Mathematical Fluid Mechanics", for inviting the manuscript to WATER. I deeply appreciate the positive critiques of three anonymous reviewers that helped considerably to straighten out the manuscript.

Conflicts of Interest: The author declares no conflict of interest.

References

1. Reeves, M.J. Recharge of the English chalk, A possible mechanism. *Eng.Geol*., **1980**, *14*, 231–240.
2. Atkinson, T.C.; Smith, D.I. Rapid groundwater flow in fissures in the chalk: An example from South Hampshire. *Q. J. Eng. Geolog.* **1974**, *7*, 197–2016.
3. Richards, L.A. Capillary conduction of liquids through porous mediums. *Physics* **1931**, *1*, 318–333.
4. Jarvis, N.; Koestel, J.; Larsbo, M. Understanding Preferential Flow in the Vadose Zone: Recent Advances and Future Prospects. *Vadose Zone J.* **2016**, *15,* doi:10.2136/vzj2016.09.0075.
5. Morbidelli, R.; Corradini, C.; Saltalippi, C.; Flammini, A.; Dari, J.; Govindaraju. R.S. Rainfall infiltration modelling. *Water* **2018**, *10*, 1873.
6. Poiseuille, J.L.M. Recherches expérimentales sur le mouvement des liquides dans les tubes de très petits diamètres. *Comptes Rendus, xi-xii, Mém. des Sav. Etrangers* **1846,** *ix*, 2.
7. Darcy, H. *Les Fontaines Publiques de la Ville de Dijon*; Dalmont: Paris, France, **1856.**
8. Dupuit, J. *Études Théoriques et Pratiques sur le Movement des Eaux Dans les Canaux Découverts et à Travers les Terrains Permeable*, 2 me Ed; Dunod: Paris, France, 1863
9. Forchheimer, P.H. Wasserbewegung durch Boden. *Zeitschr. Ver. Deutscher Ingenieure* **1901**, *45*, 1782–1788.
10. Schumacher, W. *Die Physik des Bodens*; Wiegandt & Hempel: Berlin, Germany, 1864**.**
11. Lawes, J.B.; Gilbert, J.H.; Warington, R. On the Amount and Composition of the Rain and Drainage Water Collected at Rothamsted; Williams, Clowes and Sons Ltd: London, UK, 1882.
12. Buckingham, E. *Studies on the Movement of Soil Moisture.* Bulletin 38; U.S. Department of Agriculture, Bureau of Soils: Washington, DC, USA, 1907**.**
13. Young, T. An essay on the cohesion of fluids. *Philos. Trans. R. Soc. Lond.* **1805**, *95*, 65–87.
14. Fourier, J.B.J. *Théorie Analytique de la Chaleur*; Firmin-Didot: Paris, France, 1822.
15. Ohm, G.S. Vorläufige Anzeige des Gesetzes, nach welchem Metalle die Contact Eletricität leiten. *Annalen der Physik und Chemie*. **1825**, *80*, 79–88.
16. Or, D. The tyranny of small scales on presenting soil processes in global land surface models. *Water Resour. Res*. **2018**, doi:10.1029/2019WR024846.
17. Richardson, L.F. *Weather Prediction by Numerical Process*; Cambridge University Press: Cambridge, UK, 1922**.**
18. Gardner, W.; Israelsen, O.W.; Edlefsen, N.E. and Clyde, H. The capillary potential function and its relation to irrigation practice. *Phys. Rev.* **1922**, *20*, 196.
19. Philip, J.R. Theory of infiltration. *Adv. Hydrosci.* **1969**, *5*, 215–290.

20. van Genuchten, M.T. A Closed-form Equation for Predicting the Hydraulic Conductivity of Unsaturated Soils. *Soil Sci. Soc. Am. J.* **1980**, *44*, 892–898.
21. Simunek, J.; Senja, M. and van Genuchten, M.T. HYDRUS-2D, Simulating water flow, heat and solute transport in two-dimensional variably saturated media. Version 2.0. USDA-ARS, U.S. Salinity Laboratory: Riverside, CA and International Ground Water Modeling Center: IGMC-TPS53, Colorado School of Mines, Golden, CO, USA, 1999.
22. Burger, H. Physikalische Eigenschaften von Wald- und Freilandböden. *Mitt. schweiz. Centralanstalt forstl. Vers'wesen* **1922,** *XIII*, 1–221.
23. Veihmeyer, F.J. Some factors affecting the irrigation requirements of deciduous orchards. *Hilgardia* **1927**, *2*, 190.
24. Veihmeyer, F.J. Soil Moisture. In *Handbuch der Pflanzenphysiologie*; Springer: Verlag, Heidelberg, 1954.
25. Bouma, J.; Jongerius, A.; Bursman, O.; Jager, A. and Schonderbeek, D. The function of different types of macropores during saturated flow through four swelling soil hirizons. *Soil Sci. Sco. Am. J.* **1977**, *41*, 945–950.
26. Beven, K.; Germann, P. Macropores and water flow in soils, *Water Resour. Res*., **1982**, *18*, 1311–1325.
27. Abou Najm, M.; Lassabatere, L. and Stewart, R.D. Current insights into nonuniform flow across scales, processes, and applications. *Vadose Zone J*. **2018**, *18.*
28. Beven, K. A century of denial: Preferential and nonequilibrium water flow in soils, 1864–1984. *Vadose Zone J.* **2018**, *17*, 180153.
29. Atalah, N.M.; Abou Najm, M. Characterization of synthetic porous media using non-Newtonian fluids: Experimental evidence. *Europ. J. Soil Sci*. **2018**, doi:10.1111/ejss.12746.
30. Newton, I. *The Mathematical Principles of Natural Philosophy—Translation into English,* Vol. II; Benjamin Motte: London, UK, 1729, p.184.
31. Germann, P.; Beven, K. Water flow in soil macropores. I. an experimental approach. *J. Soil Sci. (British)* **1981**, *82*, 1–13.
32. Germann, P.; Beven, K. Water flow in soil macropores. III. A statistical approach. *J. Soil Sci. (British)* **1981**, *82*, 31–39.
33. Beven, K.; Germann, P. Water flow in soil macropores. II. A combined flow model. *J. Soil Sci.(British)* **1981**, *32*, 15–29.
34. Lighthill, M.J.; Whitham, G.B. On kinematic waves I. Flood movement in long rivers. *Proc. R. Soc. London. Ser. A. Math. Phys. Sci.* **1955**, *229*, 281–316.
35. Germann, P. Kinematic wave approach to infiltration and drainage into and from soil macropores. *Trans. ASAE* **1985**, *28*, 745–749.
36. Germann, P.; Edwards, W.M.; Owens, L.B. Profiles of Bromide and Increased Soil Moisture after Infiltration into Soils with Macropores. *Soil Sci. Soc. Am. J.* **1984**, *48*, 237–244.
37. Germann, P. Rapid drainage response to precipitation. *Hydrol. Proc*. **1986**, *1*, 3–13.
38. Germann, P.; DiPietro, L.; Singh, V. Momentum of flow in soils assessed with TDR-moisture readings. *Geoderma* **1997**, *80*, 153–168.
39. Flammer, I.; Blum, A. Leiser, A. and Germann, P. Acoustic assessment of flow patterns in unsaturated soil. *J. of Applied Geophys.* **2001**, *46*,115–128.
40. Germann, P. Viscosity-the weak link between Darcy's law and Richards' capillary flow. *Hydrol. Proc*. **2018**, *32*, 1166–1172.
41. Germann, P.; Beven, K. Kinematic wave approximation to infiltration into soils with sorbing macropores. *Water Resour. Res.* **1985**, *21*, 990–996.
42. Germann, P.; Helbling, A.; Vadilonga, T. Rivulet Approach to Rates of Preferential Infiltration. *Vadose Zone J.* **2007**, *6*, 207–220.
43. Kutilek, M.; Germann, P. Converging hydrostatic and hydrodynamic concepts of preferential flow definitions. *J. Contam. Hydrol.* **2009**, *104*, 61–65.
44. Germann, P. *Preferential Flow—Stokes Approach to Infiltration and Drainage***, 2014,** University of Bern: Bern, Switzerland. Available online: https://boris.unibe.ch/119081/1/preferential_flow.pdf.
45. Germann, P. Preferential flow at the Darcy scale: Parameters from water content time series. *Methods Soil Anal.* **2018**, *3*, 160121.
46. Germann, P.; Karlen, M. Viscous-flow approach to in situ infiltration and in vitro saturated hydraulic conductivity determination. *Vadose Zone J.* **2016**, *15*, doi:10.2136/vzj2015.05.0065.

47. Selker, J.; Parlange, J.-Y.; Steenhuis, T. Fingered flow in two dimensions: 2. Predicting finger moisture profile. *Water Resour. Res.* **1992**, *28*, 2523–2528.
48. Germann, P.; al Hagrey, S.A. Gravity-driven and viscosity-dominated infiltration in a full-scale sand model. *Vadose Zone J.* **2008**, *7*, 1160–1169.
49. Germann, P.; Prasuhn, V. Viscous flow approach to rapid infiltration and drainage in a weighing lysimeter. *Vadose Zone J.* **2018**, *17*, 170020.
50. Rimon, Y.; Dahan, O.; Nativ, R.; Geyer. S. Water percolation through a deep vadose zone and groundwater recharge: Results based on a new vadose zone monitoring system. *Water Resour. Res.* **2007**, 43: W05402.
51. Hincapié, I.A.; Germann, P. Abstraction from Infiltrating Water Content Waves during Weak Viscous Flows. *Vadose Zone J.* **2009**, *8*, 996–1003.
52. Demand, D.; Blume, T. and Weiler, M. Spatio-temporal relevance and controls of preferential flow at the landscape scale. *Hydrol. Earth Syst. Sci.* **2019**, *23*, 4869–4889.
53. Blum, A.; Flammer, I.; Friedly T.; Germann, P. Acoustic tomography applied to water flow in unsaturated soils. *Vadose Zone J.* **2004**, *3*, 288–299.
54. Germann, P.; Jäggi; E.; Niggli, T. Rate, kinetic energy and momentum of preferential flow estimated from in situ water content measurements. *Europ. J. Soil Sci.* **2002**, *53*,607–617.
55. Germann, P.; Hensel, D. Poiseuille flow geometry inferred from velocities of wetting fronts in soils. *Vadose Zone J.* **2006**, *5*, 867–876.
56. Hincapié, I.; Germann, P. Water Content Wave Approach Applied to Neutron Radiographs of Finger Flow. *Vadose Zone J.* **2010**, *9*, 278–284.
57. Dubois, J.-D. *Typologie des aquifers du cristallin: Exemples des massifs des Aiguilles Rouges et du Mont-Blanc.* 1991 *(*Typology of Aquifers in the Cristaline: Examples from the Massifs Aguilles Rouges and Mt. Blanc). Ph.D. Dissertation, Department of Civil Engineering, EPFL, Lausanne, Switzerland. Available online: https://www.swisstransfer.com/d/1442dd60-cf83-4220-a8e0-01e30bd5e34f (accessed on 22 January 2020).
58. Germann, P. Hydromechanics and kinematics in preferential flow. *Soil Sci.* **2018**, *183*, 1–10.
59. Hincapié, I.; Germann, P. Impact of initial and boundary conditions on preferential flow. *J. Contam. Hydrol.* **2009**, *104*, 67–73.
60. Larsbo, M.; Koestel, J.; Jarvis, N. Relations between macropore network characteristics and the degree of preferential solute transport. *Hydrol. Earth Syst. Sci.* **2014**, *18*, 5255–5269.
61. Bogner, C.; Germann, P. Viscous flow approach to "pushing out old water" from undisturbed and repacked soil columns. *Vadose Zone J.* **2019**, *18*, 180168.
62. Germann, P.; Alaoui, A.; Riesen, D. Drag force approach to the transport of colloids in unsaturated soils. *Water Resour. Res.* **2002**, *38*, 18–1.
63. Bigalke, M.; Montserrat, F. Foreword to the research front on 'Microplasitcs in Soils'. *Environ. Chem.* **2019**, *16*,1–2.
64. Yu, M.; van der Ploeg, M; Lwanga, E.H.; Yang, X.; Zhang, S.; Ma, X; Ritsema, C.J. and Geissen, V. Leaching of microplastics by preferential flow in earthworm (*Lumbricus terrestris)* burrows. *Environ. Chem.* **2019**, *16*, 31–40.
65. Lange, B.; Lüscher, P.; Germann, P.F. Significance of tree roots for preferential infiltration in stagnic soils. *Hydrol. Earth Syst. Sci.* **2009**, *13*, 1809–1821.
66. Wiekenkamp, I.; Huisman, J.A.; Bogena, H.R.; Vereecken, H. Effects of deforestation on water flow in the vadose zone. *Water* **2020**, *12*, 35.